Biogeochemistry **61:** 95–113, 2002.

Under-ice CO_2 and O_2 variability in a freshwater lake

MATTHEW M. BAEHR[1,2] and MICHAEL D. DEGRANDPRE[1,*]
*[1]Department of Chemistry, The University of Montana, Missoula, MT 59812, USA; [2]Current address: Large Lakes Observatory, University of Minnesota, 10 University Dr., 109 RLB, Duluth, MN 55812, USA; *Author for correspondence (e-mail: mdegrand@selway.umt.edu)*

Received 12 April 2001; accepted in revised form 25 September 2001

Abstract. Autonomous, in situ sensors for the partial pressure of CO_2 (pCO_2) and dissolved oxygen (DO) were deployed in a freshwater lake during the winters of 1997 and 1998 to evaluate magnitude and sources of variability during ice-covered periods. Gas variability on diel or shorter time scales was small or undetectable during most of the deployment periods, only becoming significant prior to ice-out when runoff and light penetration increased, promoting convective currents and biological production. A surprising 7.6 d period oscillation, apparently driven by a baroclinic seiche, dominated the short-term variability during the first year. The gas trends associated with the seiche oscillations and periodic profile measurements revealed that ice formation led to gas gradients directly under the ice. Long-term variability was characterized by increasing CO_2 and decreasing DO as a consequence of biological oxidation of organic matter. The results suggest that both spatial and temporal variability can be significant over intervals which would not be resolved by traditional sampling-based studies.

Introduction

Lakes undergo dramatic changes in physical forcings between ice-covered and ice-free periods with important consequences for seasonal biogeochemical cycles. Ice insulates the lake from wind-generated mixing, gas and heat exchange, and light penetration. The duration of ice-cover has been shown to be important in determining seasonal dissolved O_2 (DO) levels (e.g., Schindler (1971); Schindler et al. (1974); Mathias and Barica (1980); Babin and Prepas (1985); Baird et al. (1987); Livingstone (1993)), partial pressure of CO_2 (pCO_2) supersaturation (e.g., Coyne and Kelley (1974); Hesslein et al. (1991); Cole et al. (1994); Striegl and Michmerhuizen (1998)) and water column pH (Kratz et al. 1987). While seasonal trends have been well characterized, little is known about short-term biogeochemical variability in ice-covered lakes. A number of processes can act over short time periods, such as convective mixing from light penetration (Nebaeus 1984; Kling et al. 1992; Bengtsson 1996), which could potentially influence short-term and seasonal biogeochemical cycles. Our objective in the present study has been to define important temporal scales of biogeochemical variability and determine their relationship to physical processes during ice-covered periods by taking advantage of state-of-the-art in situ chemical sensor technologies.

We used sensors for pCO_2 (DeGrandpre et al. 1995) and DO (YSI, Inc.) deployed under ice to collect the in situ time-series. The studies were conducted in

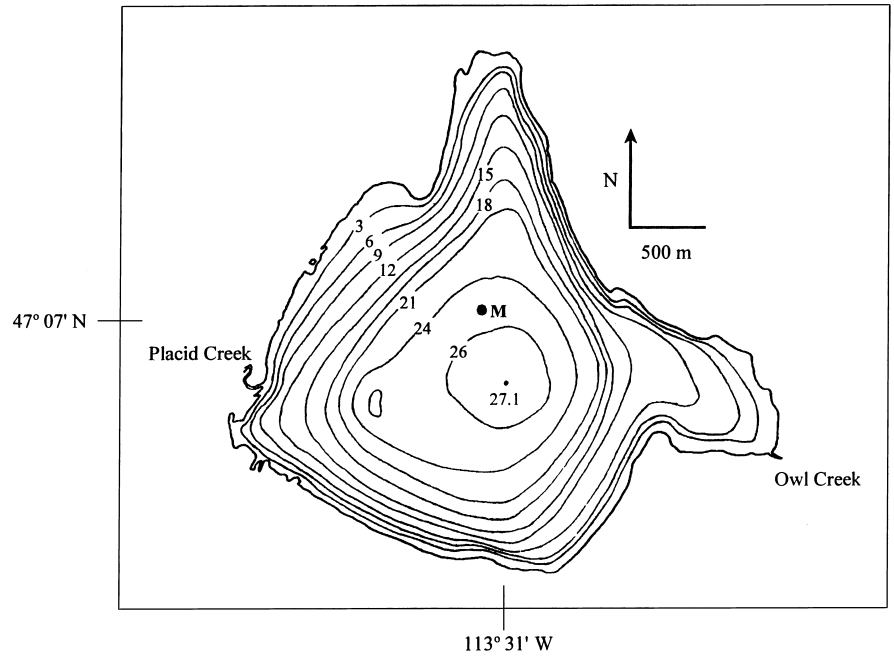

Figure 1. Bathymetric map of Placid Lake, Montana. M designates the location of the instrumented mooring(s) deployed during 1997 and 1998. Contours are in meters.

Placid Lake, Montana USA during the winters of 1997 and 1998. Data from periodic sampling and regional meteorological stations are also used to aid interpretation of the in situ data.

Methods

Study lake

Studies were conducted on Placid Lake (47°07′ N, 113°31′ W), 45 km NE of Missoula, Montana (Figure 1). Placid Lake is a dimictic, mesotrophic lake (Juday and Keller 1980) that resides in a sedimentary carbonate rock basin at an elevation of 1256 m (Streebin et al. 1973). The lake has a surface area of 4.90×10^6 m^2, volume of 7.33×10^7 m^3, maximum depth of 27.1 m, and a mean depth of 15.0 m. Placid Creek, which drains an area of 180.3 km^2, is the primary surface water source (Figure 1) (Streebin et al. 1973). The hydrologic residence time of the lake, determined from discharge measurements made on Placid Creek and the outlet stream (Owl Creek), is $\sim$2 years. Local groundwater input into the lake is considered negligible (Juday and Keller 1980), a finding supported by discharge measurements performed by our group.

Table 1. In situ instrumentation deployed under ice on a subsurface mooring in 1997 and 1998. Instrument descriptions are given in the text. The depth is the initial deployment depth.

Instrument	Parameters	Accuracy	Resolution	Instrument deployment periods	Depth (m)
SAMI-CO_2	pCO_2	See text	See text	Jan. 8–May 29, 1997 (1)[a]	2.7
	Temperature	0.15 °C	0.01 °C	Nov. 26, 1997–May 20, 1998 (1)	3.2
YSI Inc.	O_2	0.20 mg L^{-1}	0.01 mg L^{-1}	Jan. 8–May 29, 1997 (2)	2.9
Model 6000	Temperature	0.15 °C	0.01 °C	Nov. 26, 1997–May 20, 1998 (1)	3.4
	Conductivity depth		0.01 mS cm^{-1}	March 14–May 12, 1998 (1)[b]	2.4
LI-COR Inc.	PAR			Jan. 8–May 29, 1997 (1)	1.5
Model LI-192SA				Nov. 26, 1997–May 20, 1998 (1)	2.0
Onset Computer Corp. Model WTA080537	Temperature	0.20 °C	0.15 °C	March 14–May 12, 1998 (5)[b]	1.0, 2.0, 3.0, 4.0, 5.0

[a] The number of instruments deployed for the period.
[b] This deployment was made on a second subsurface mooring.

Mooring detail

A subsurface mooring was placed near the center of Placid Lake at 25 m depth (Figure 1). In situ sensors for pCO_2, DO, photosynthetically active radiation (PAR), temperature and depth (pressure) were deployed on the mooring. The instrumentation deployment periods and depths are presented in Table 1. All biogeochemical instrumentation was located near the surface, the expected zone of greatest short-term variability. Instrument availability prohibited more extensive spatial coverage. All instruments were programmed to acquire data every half-hour. An additional mooring equipped with a thermistor chain and a DO sonde was deployed in winter 1998 (Table 1).

In situ chemical measurements

The moored pCO_2 measurements were made using the Submersible Autonomous Moored Instrument for CO_2 (SAMI-CO_2) described in DeGrandpre et al. (1995, 1997). The SAMI-CO_2 was calibrated prior to deployment using CO_2 gas standards (DeGrandpre et al. 1997). Measurement precision, estimated from the SAMI-CO_2 calibrations, is $\sim$ ±1 μatm at 360 μatm, ±10 μatm at 1200 μatm, and ±20 μatm at 1500 μatm. Accuracy prior to deployment is $\sim$ ±1–3 μatm at 360 μatm and is estimated to be similar to the precision at higher levels. The increasing uncertainty reflects the decrease in sensitivity at higher pCO_2 levels (DeGrandpre et al. 1999). A single SAMI-CO_2 was located as close to the surface as possible during both years of the study (Table 1). Data accuracy during the deployment was evaluated through periodic measurements of total dissolved inorganic carbon (DIC) and pH, discussed in detail below.

DO was measured with commercially available autonomous sondes (YSI, Inc., Model 6000). The reported sensor precision is ±0.3 μmol L^{-1}. Single-point DO calibrations were performed in water-saturated air at 4.0 °C just prior to deployment. During most of the deployment periods, two Model 6000's were deployed at the same depth to provide in situ replicates (Table 1). These data, along with comparisons to the in situ pCO_2, were used to evaluate the drift and, hence, accuracy of the in situ DO measurements (discussed below).

Other in situ measurements

PAR (waveband 400 to 700 nm) was measured with an underwater quantum sensor (LI-COR, Inc., Model LI-192SA) connected to an external sensor input on the SAMI-CO_2. Temperature (±0.01 °C, SAMI-CO_2 and Model 6000), conductivity (±0.001 mS cm^{-1}, Model 6000), and depth (±0.001 m, Model 6000) were also recorded. The additional mooring deployed in 1998 had internally-logging thermistors (Onset Computer Corp., Model WTA080537) located at 1 m intervals from 1 to 5 m (Table 1).

Periodic profile samples

Samples for DIC and pH were obtained with a Kemmerer sampler at 2, 5, 10, 15, and 20 m depths on 8 Jan, 3 Feb, 23 Feb, and 17 Mar in 1997 and on 9 Feb and 3 Mar in 1998. Analyses were performed on replicate samples obtained from two different casts. Samples were transferred to acid-washed 500 ml glass bottles using care to limit gas exchange. The samples were analyzed for DIC in the laboratory within 24 hr using a DOC/DIC carbon analyzer (Shimadzu Corp., Model TOC5000A). The analyzer was calibrated with three freshly prepared Na_2CO_3/$NaHCO_3$ standards that bracketed the sample concentration. The mean precision for the DIC method, based on three intra-sample measurements, was typically ±0.5% ($\sim$±6 μM) and the agreement between the two separate casts at each depth was typically within ±1% of the mean.

Sample pH was determined within 24 hr using a spectrophotometric method developed for seawater pH (Byrne and Breland 1989). This method was selected over conventional glass pH electrodes because of the well-known junction potential error that occurs in low ionic strength samples (e.g., Brezinski (1983); Herczeg and Hesslein (1984)). The spectrophotometric method has excellent reproducibility (±0.005 pH unit intra sample and ±0.01 pH unit between two casts at the same depth); however, uncertainty in the indicator equilibrium constant (pK_a), along with the pH perturbation caused by addition of the indicator, result in an uncertainty in the absolute pH (French et al. 2002). To account for the systematic uncertainty in the pH method, a constant offset was applied to the pCO_2 calculated from the DIC and pH measurements (also discussed below).

Total alkalinity and CO_2 calculations

The periodic pH and DIC measurements were used to estimate total alkalinity (TA) and to verify the long-term stability of the in situ pCO_2 measurements. TA was used as a quasi-conservative tracer to convert the pCO_2 records into DIC for estimates of CO_2 accumulation rates, as presented below. An in-house QuickBasic (Microsoft Corp.) program was used for all calculations. The carbonate dissociation constants at infinite dilution were obtained from Millero (1979) and the CO_2 solubility-temperature relationship from Weiss (1974). These calculations assume TA is 100% carbonate alkalinity; this assumption is supported by subsequent Placid Lake measurements in which the carbonate system was over-determined (Baehr 2000).

Other supporting data

Daily high and low temperature and total daily precipitation were obtained from the USDA Forest Service Seeley Lake Ranger District Station on Seeley Lake, 10 km N of Placid Lake. Wind speed and barometric pressure were obtained from a NOAA National Data Center site at Johnson-Bell Field in Missoula, Montana. Discharge data were obtained for the Swan River (USGS Station 12370000) in the Swan drainage $\sim$32 km N of Placid Lake, the nearest gauging station to Placid Lake.

Results

Conditions during winter 1997 and 1998

Ice cover records from USDA Forest Service personnel for Seeley Lake, which often freezes and thaws within a few days of Placid Lake (E. Keller, pers. comm.), were used to estimate periods of Placid Lake ice cover. Based on these observations, ice cover lasted from $\sim$ 12 Dec 1996 to 19 Apr 1997 for a total of 128 days.

Ice cover was 11 days shorter in the second study year, extending from ~ 19 Dec 1997 to 15 Apr 1998.

1997 and 1998 in situ time-series

The pCO_2, DO, temperature, light, and mooring depth time-series are shown in Figures 2 and 3. Data gaps are present because of periodic instrument malfunction. During Year 1, the pCO_2 ranged from ~1020 to 1660 μatm or ~3 to 5 times atmospheric saturation (~320 μatm at the local average barometric pressure). In Year 2 the pCO_2 ranged from ~1420 to 1700 μatm. The pCO_2's calculated from DIC and pH are also shown in Figures 2a and 3a. The large disagreement with the first profile measurement (Figure 2a) is believed to be an artifact of the sampling method on that day when deeper samples were obtained first, thereby entraining deeper, higher pCO_2 water to the surface. Omitting the first profile measurement, the agreement in Year 1 was ±19 μatm (N=3). The validity of the DIC/pH calculations and use of the constant offset are further supported by Year 2 comparisons. The calculated pCO_2, with the same offset as in Year 1, agreed to within ±29 μatm (N=2) of the in situ pCO_2 (Figure 3a). The calculated pCO_2 suggests that there was minimal drift in the in situ pCO_2 measurements, as found in earlier studies (DeGrandpre et al. 1995, 1998). In addition, post-calibration of the SAMI-CO_2 during Year 1 verified that drift was <3.5%. This drift is an upper bound estimate because the post-calibration was not performed until after the instrument was recovered, nearly 2 months after the data reported in Figure 2. No post-calibration was possible for Year 2 because of an instrument malfunction. Both the magnitude and trends in the pCO_2, and its relationship with DO, are consistent with other researcher's observations during ice-cover (e.g., Wetzel (1983); Cole et al. (1994)), further supporting that there was minimal drift in the measurements.

During Year 1, DO ranged between 75–69% saturation and during Year 2 from 70–63% saturation. Comparison of the replicate DO records, obtained at similar depths (Table 1), was used to verify the quality of the DO data. Only one of the two DO sensor records is shown (Figures 2b and 3b). In Year 1 the DO sensor records initially had large and erratic offsets, however they converged later in the deployment, matching to within ±6 μmol L^{-1} (N=1920). The DO data are shown only for this time period and are assumed to be accurate to within ±6 μmol L^{-1}. In addition, as stated above, the Year 1 DO record is also consistent with trends in the pCO_2 data, further supporting that there was minimal drift in the DO measurements. In Year 2, the main mooring DO record agreed with the additional Model 6000 deployed on the thermistor-chain mooring to within ±3 μmol L^{-1} (N=1266) later in the field study (Table 1). Earlier in the record there were significant erratic offsets. Data are omitted during these time periods. We believe the erratic behavior of the Model 6000's was a result of the relatively old electrodes (3 years) that were used in the study.

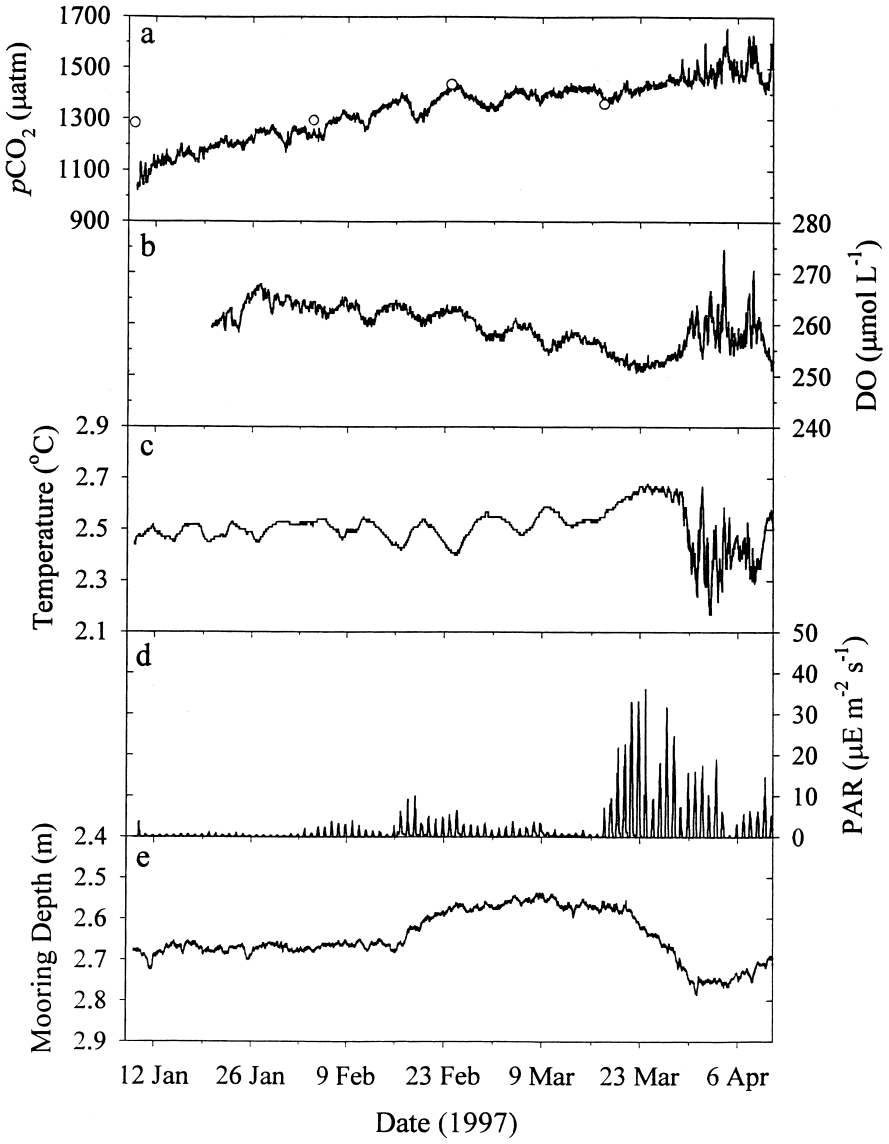

Figure 2. Under-ice in situ time-series collected during Year 1. Instrumentation and their deployment periods are given in Table 1. a) In situ pCO_2 (line) and pCO_2 calculated from the periodic DIC and pH samples (open circles). A constant offset of – 149 μatm was applied to the calculated pCO_2. b) Dissolved oxygen. The saturation level at 2.5 °C is 366.9 μmol L^{-1}. c) Water temperature at the instrument depth. d) Photosynthetically active radiation (PAR). e) Depth of the moored instrumentation. All times are UTC.

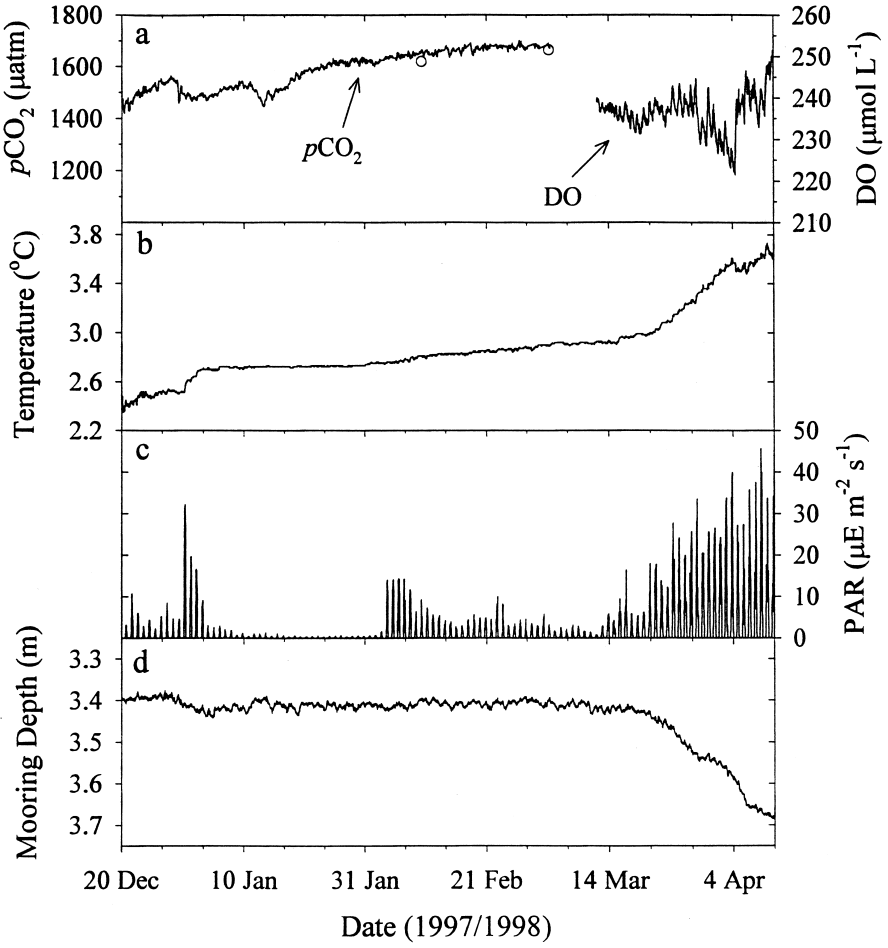

Figure 3. Under-ice in situ time-series collected during Year 2. a) The pCO_2 and DO records. The open circles are the pCO_2 calculated from the periodic DIC and pH samples. A constant offset of – 149 μatm was applied to the calculated pCO_2. b) Water temperature at the instrument depth. c) Photosynthetically active radiation. d) Depth of the moored instrumentation relative to the lake surface.

Discussion

Temporal scales of variability

Much of the diel and shorter time scale variability was smaller than the resolution of the in situ instruments, as noted by the digitized appearance of the DO and temperature data in Figure 2. The greatest short-term variability occurred during the period prior to ice-out (Mar/Apr). Clear oscillations and long-term trends are also evident. The large range of temporal scales of variability suggests that multiple

processes contribute to variability under ice. Our evaluation first focuses on the variability in Year 1 followed by a comparison with the Year 2 time-series data.

Year 1

The most striking feature during Year 1 was the low frequency oscillation common in the pCO_2, DO, and water temperature time-series (Figure 2). The oscillations in the three records have the same period, 7.6 ± 1.8 days. The consistent period suggests that the oscillations were driven by a seiche. Wind has been found to induce internal seiche in ice-covered lakes through forcing of the ice-cover (Bengtsson 1996; Malm et al. 1998) although, to our knowledge, low frequency oscillations in biogeochemical properties under ice have never been observed. The oscillations began to develop around 12 Jan 1997 based on the temperature record (Figure 2c) coincident with a high wind event with wind speeds over 11 m s^{-1} and an average of 7.5 m s^{-1} over a 24 hr period (Figure 4b). The long period of the oscillations and the presence of very weak density stratification (Figure 6) point to a baroclinic seiche (Malm et al. 1998). The period of a baroclinic seiche can be predicted using:

$$T_n = \frac{2n\pi L}{NH} \tag{1}$$

when n = number of the baroclinic mode, L = maximum length of the lake basin, H = mean depth of the lake minus the ice thickness, and N = buoyancy frequency, given by

$$N^2 = \frac{gd\rho}{\rho dz} \tag{2}$$

where g = gravity acceleration, ρ = average water density (999.957 kg m^{-3}), and $d\rho/dz$ is the average vertical density gradient (Malm et al. 1998). Both ρ and $d\rho/dz$ were estimated from the temperature profiles shown in Figure 6. Under these conditions, the period of the first baroclinic mode would be 5.5 days which, considering the large uncertainty inherent in this calculation, compares well with the observed 7.6 day period. These results strongly suggest that the oscillations were seiche-driven. The high winds on 12 Jan may have initiated the seiche and subsequent prevailing winds or other episodic events (Figure 4) presumably acted to sustain the seiche at this resonant frequency of the lake. A seiche-induced sloshing should also result in an oscillating depth, but this was not observed (Figure 2e). However, if the instruments were at the node of the seiche, which would be near the center of the lake where the mooring was located, no depth change would be apparent (Wetzel 1983; Lemmin 1987). Other possible mechanisms are unlikely and are not supported by the data. For example, episodic storms, which pass through the area (see meteorological data in Figure 4), could also create a low periodicity variability, however, no correlation was found between these events and the dis-

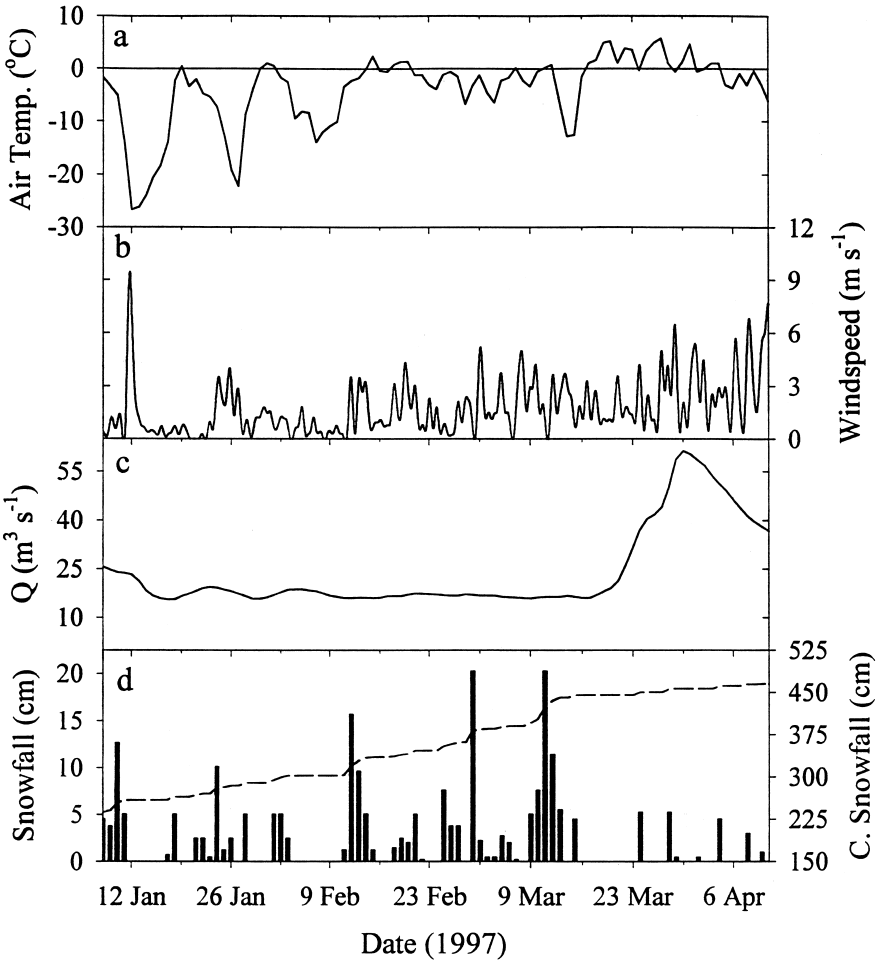

Figure 4. Year 1 meteorological and discharge data. a) Average of daily high and low air temperatures 10 km N of Placid Lake. b) Wind speed, measured at the NOAA site in Missoula, Montana, 24 hr low-pass filtered for clarity. c) USGS Swan River discharge record. The discharge pattern for this river is used as a proxy for the discharge pattern of Placid Creek. d) Total daily snowfall (bars) and cumulative snowfall from ice-up (dashed line) 10 km N of Placid Lake.

solved gas oscillations (R^2<0.2). In addition, power spectra of barometric pressure, wind, and air temperature did not show a peak at 7.6 days.

The higher pCO_2 and higher DO water associated with the oscillations is also an unusual feature. The pCO_2 and DO are positively correlated within the 7.6 days period (R^2=0.88), whereas, in most aquatic ecosystems the biological imprint creates a negative correlation. Looking closely at Figures 2a–2c, one can see that the rising pCO_2 and DO levels are associated with slightly colder and less dense water (T < 4 °C). As can be seen in Figure 6, water temperature decreased towards the ice-water interface suggesting that the water originated from closer to the surface.

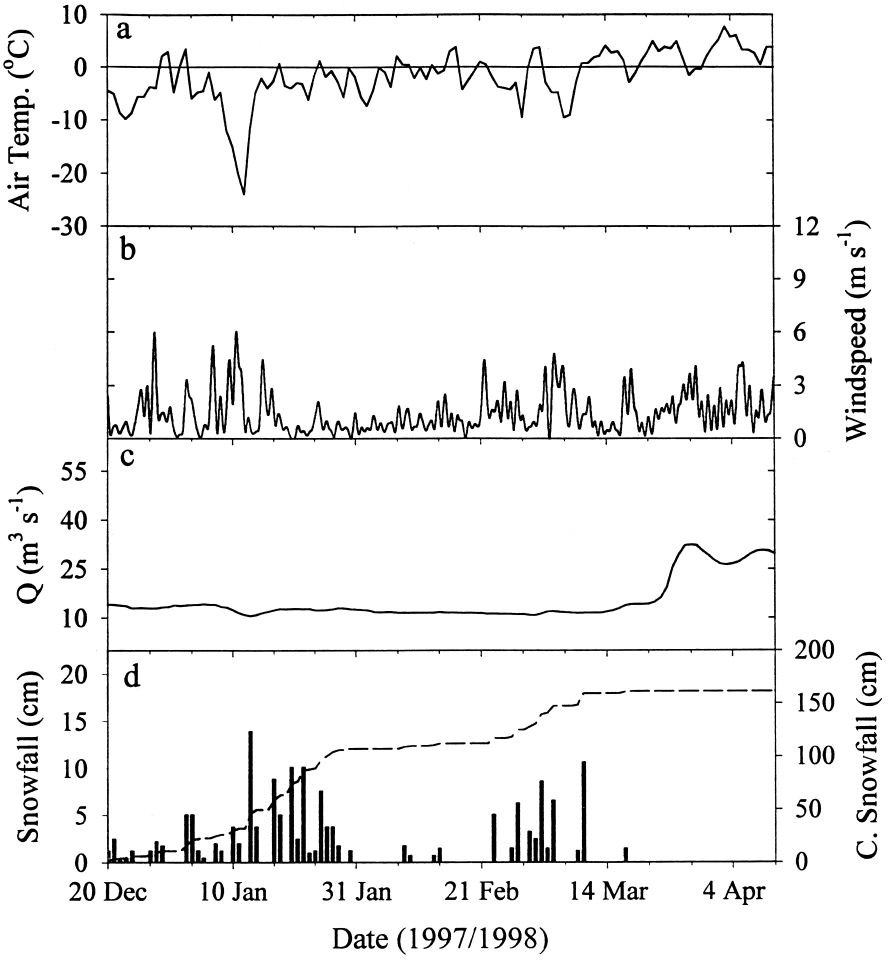

Figure 5. Year 2 meteorological and discharge data. Detail as in Figure 4.

Gases and other solutes are known to partition into the liquid phase when ice forms (Bari and Hallett 1974; Welch and Bergmann 1985; Craig et al. 1992). This process would result in an increase in DIC and DO in the colder water above the instrumentation. DIC profile measurements and isopleths (Figures 7a and 8) show that DIC increased near the ice surface during the ice covered period. Because no significant vertical movement of water was evident, surface DIC, and as a result, pCO_2, along with O_2 must vary along the surface of the lake. Horizontal gradients could arise from variable ice thickness (Stigebrandt 1978) with correspondingly different concentrations of dissolved solutes.

Higher frequency variability became significant prior to ice-out. As shown in Figures 2 and 9, pCO_2, DO, and temperature were more variable relative to earlier in the record. Late in the ice-covered period light penetration increased (Figure 2).

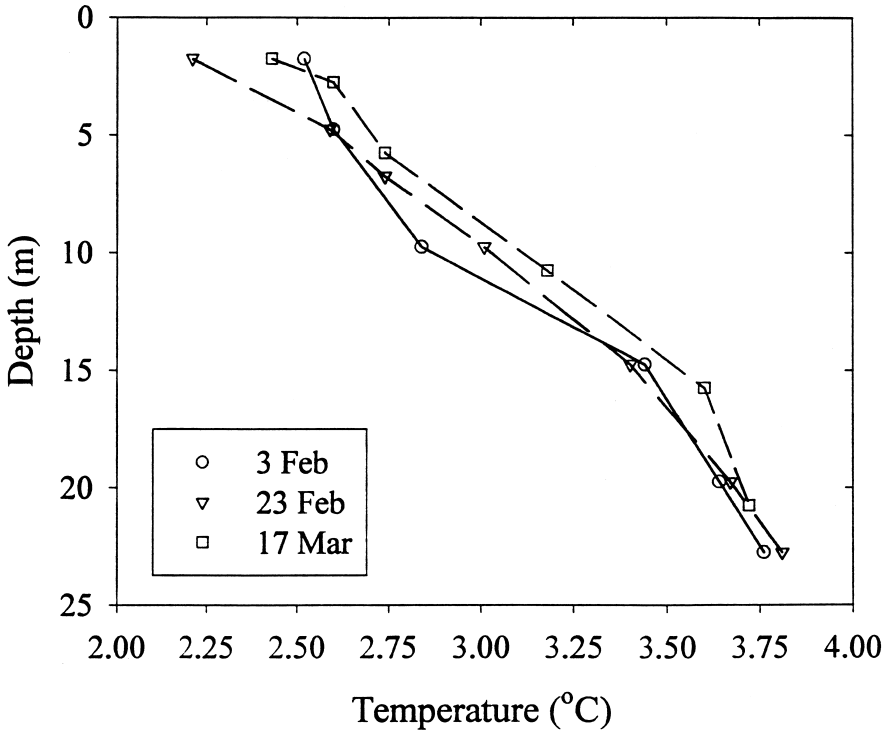

Figure 6. Under-ice temperature (°C) profiles measured during the Year 1 study.

Meltwater also increased, based on the colder temperatures, increased mooring depth, and dramatic rise in river discharge (Figures 2 and 4). The pCO_2 and DO are not significantly correlated (R^2=0.20) during this time period. DO is negatively correlated with temperature, i.e., higher DO in colder water, over the first 7 days of this period (R^2=0.93). Their relationship becomes unclear later (R^2=0.36 for the entire period in Figure 9). After ice-out a thin layer ($\sim$ 1 m) of colored dissolved organic matter (CDOM) was present on the lake surface which apparently originated from the inlet, Placid Creek. We observed that the runoff water was highly colored relative to the lake. Others have found that cold (<4 °C), low density stream water can fan out at the ice-water interface rather than mixing with the whole water column at the stream inlet (Bengtsson 1996). Much of the variability during the late-ice period probably resulted from mixing of the cold runoff water with resident water. Since the surface water end-member composition was unknown, we were unable to separate local variability (e.g. biological production) from advective influences. In the second year of the study, discussed below, runoff was substantially reduced and diel variability was more evident.

The long-term variability was dominated by a slow increase and decrease in the pCO_2 and DO levels, respectively (Figure 2). These trends are commonly observed in ice-covered lakes and are generally attributed to bacterial oxidation of particu-

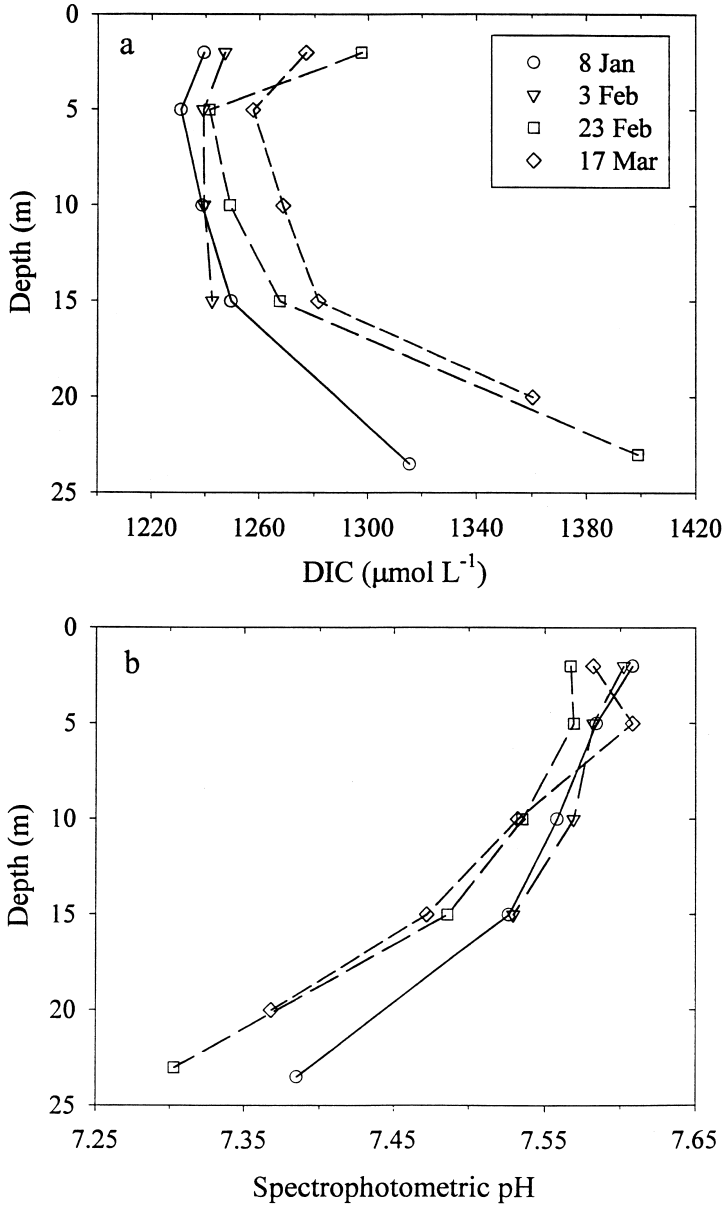

Figure 7. DIC and pH profiles obtained during Year 1. a) Dissolved inorganic carbon (DIC). b) Spectrophotometric pH. Legend is the same for both figures.

late and dissolved organic matter (e.g., Babin and Prepas (1985); Cole et al. (1994)). Respiration rates were determined by calculating the average rate of change of DIC from the pCO_2 time-series and calculated TA. The data were 20-day low-pass filtered to remove short-term variability so that a more accurate estimate of the un-

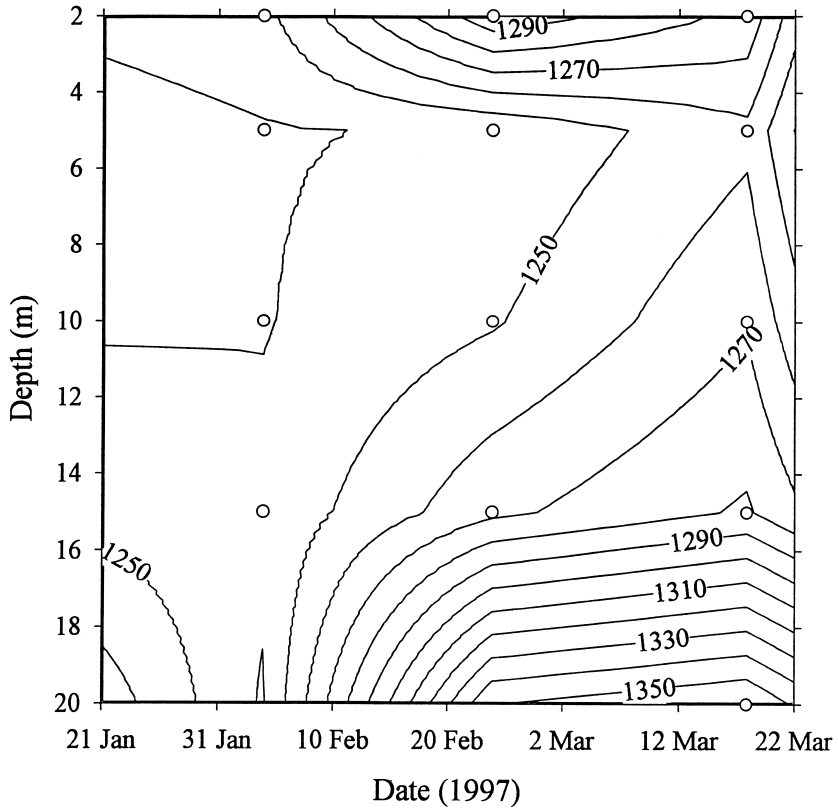

Figure 8. Year 1 DIC isopleths. Contour labels are in μmol L^{-1}. Contour interval lines were produced from linear interpolation (both time and depth) of the profiles. The jagged appearance of the contours results from interpolation between large data gaps. The open circles indicate the time and depth of the profile measurements.

derlying respiration rate could be determined. Using the filtered data, the average rate of change for DIC and DO over the period 31 Jan to 17 Mar 1997 was +0.25 ±0.21 and −0.22 ±0.14 mmol m^{-3} day^{-1}, respectively. These rates are consistent with the approximate 1:1 molar ratio of CO_2 release and DO consumption resulting from respiration of organic matter (Wetzel 1983). The rate of DO depletion on an areal basis, calculated from the 3 DIC profiles (Figure 7a) by assuming a 1:1 molar ratio was found to be −16 mmol O_2 m^{-2} d^{-1} which is within the range of DO depletion rates reported for other lakes during ice-covered periods (Babin and Prepas 1985). The respiration also had a significant impact on pH, especially in the bottom water where pH decreased by nearly 0.1 pH unit (Figure 7b).

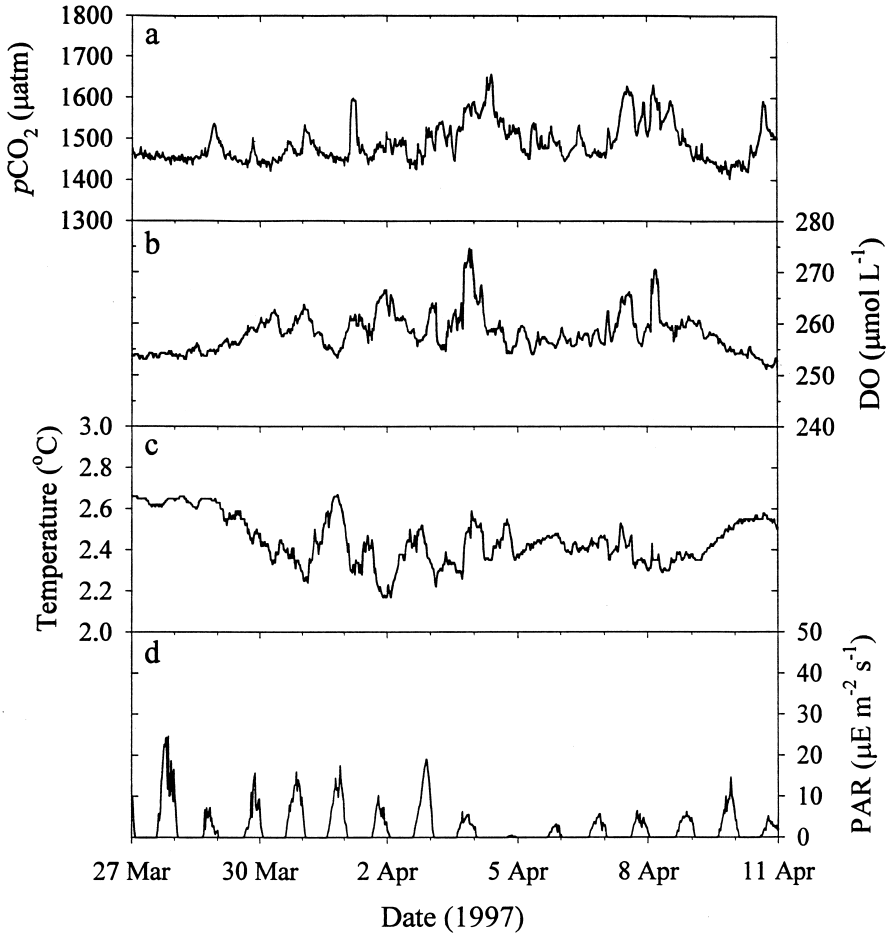

Figure 9. Expanded time-series for the late-ice period in Figure 2. a) pCO_2. b) DO. c) Water temperature. d) PAR.

Year 2

The Year 2 time-series are discussed to provide a context for the variability observed in Year 1. This ice-covered period was characterized by greater light penetration and warmer and less variable water temperatures than in Year 1 (Figure 3). The overall pCO_2 trend is strikingly similar to Year 1 with increasing pCO_2 through mid-winter, leveling off later in the ice-covered period. In contrast to Year 1, however, no low frequency oscillations were observed.

Once again short-term variability was greatest just prior to ice-out as shown by the DO record from Mar–Apr (Figures 3a and 10a) however, a clear diel cycle is present in Year 2. The DO peaks follow peaks in PAR (Figure 10) suggesting that under-ice biological production was the primary forcing. The mean rate of "pro-

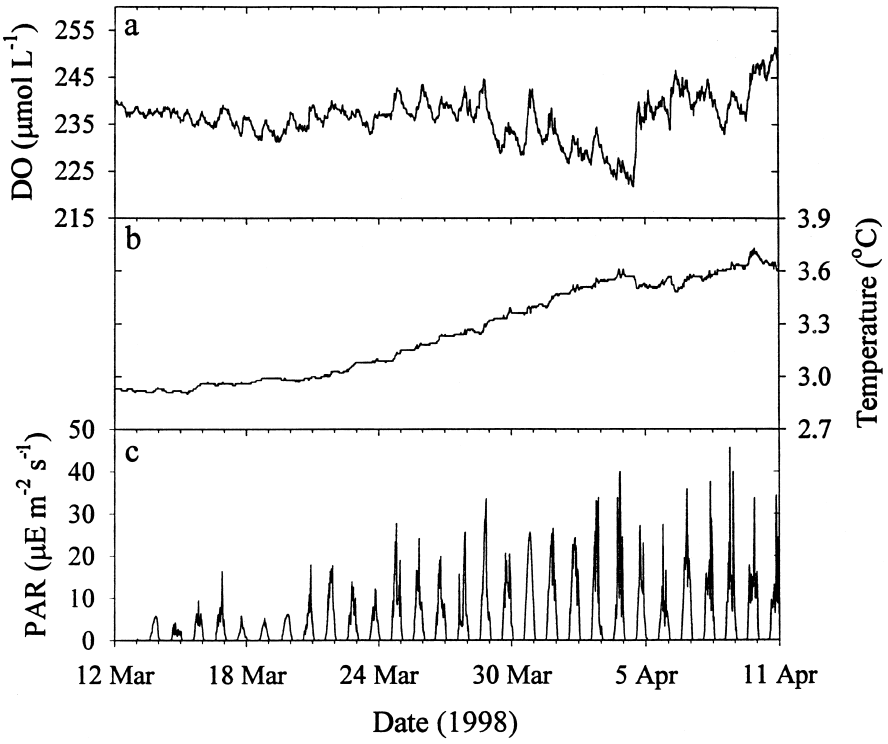

Figure 10. Expanded time-series for the late-ice period in Figure 3. a) DO. The saturation level at 3.3 °C is to 359.4 μmol L^{-1}. b) Water temperature. c) PAR.

duction", calculated from the rate of change of DO, was found to be 4.0 mmol carbon m^{-3} d^{-1}. We cite this number because almost no biological production data exist for lakes during the late-ice period. However, based on the temperature record, convective mixing could also contribute to the diel variability. The stepwise appearance of the temperature record (Figure 10b) originates from solar-driven penetrative convection of sub 4 °C water (Farmer 1975; Matthews and Heaney 1987) and the retention of heat at night because of the insulating ice cover. As explained for the Year 1 data, DO accumulates at the ice-water interface from ice formation. Convective mixing of this surface water downward would therefore lead to a daytime increase of DO at the depth of the instrumentation. A complementary pCO_2 record would have helped decipher contributions from biological and physical processes but without this information, or additional vertically-distributed sensors, their relative contributions can not be quantified.

Lastly, as stated above, the overall trend shows that pCO_2 initially increased rapidly and then leveled off. Other studies have shown that DO depletion rates are more rapid early in the under-ice period (e.g., Schindler (1971); Babin and Prepas (1985); Baird et al. (1987)). To obtain respiration rates, the pCO_2 was converted to DIC and filtered as for Year 1. The average rate of change of DIC from 15 Jan to

1 Mar was +0.26 ±0.28 mmol m^{-3} day^{-1}, similar to the Year 1 rate. Over the entire pCO_2 record the rate is +0.17 ±0.24 mmol m^{-3} day^{-1}, reduced by the two large drops in pCO_2 (Figure 3a). Comparison of the saturation levels of pCO_2 and DO during Years 1 and 2 suggests that greater respiration of organic material occurred during Year 2. The large snowfall and high runoff in Year 1, as shown in Figure 4, resulted in a large input of terrestrial organic matter. Therefore, there was increased oxygen demand in the lake during Year 2, which resulted in higher levels of pCO_2 and lower DO.

Summary and conclusions

These studies provide a detailed characterization of short and long term pCO_2 and DO variability under ice. The high resolution time-series indicate that respiration of accumulated organic matter dominated the overall trend. Physical mechanisms, which played an important secondary role, included seiche-induced advection, vertical convection from solar heating, and stream flow-through at the surface just prior to ice-out. Ice formation led to an accumulation of dissolved gases just under the ice, which uniquely manifested itself in the seiche oscillations. During the late-ice periods light penetration may have stimulated biological production but rates could not be directly estimated because the variability was convolved with physical processes. The results suggest that both spatial and temporal variability can be significant over intervals which would not be resolved by traditional sampling-based studies. Further refinement of applications that utilize new autonomous biogeochemical sensors will undoubtedly advance our understanding of the relationships between physical processes and biogeochemical cycles in aquatic ecosystems.

Acknowledgements

We would like to thank Terry Hammar (Woods Hole Oceanographic Institution), Creighton Wirick (Brookhaven National Laboratory) and Ed Keller (The University of Montana) for their assistance on this project. Funding was provided from MONTS-EPSCoR (Grant 292144) and NSF-Ocean Sciences (OCE-9814388).

References

Babin J. and Prepas E.E. 1985. Modelling winter oxygen depletion rates in ice-covered temperate zone lakes in Canada. Can. J. Fish. Aquat. Sci. 42: 239–249.

Baehr M.M. 2000. *In situ* chemical sensor measurements in a freshwater lake: An analysis of the short-term and seasonal effects of ice cover, ice out, and turnover on CO_2 and O_2. PhD Dissertation, The University of Montana.

Baird D.J., Gates T.E. and Davies R.W. 1987. Oxygen conditions in two prairie pothole lakes during winter ice cover. Can. J. Fish. Aquat. Sci. 44: 1092–1095.

Bari S.A. and Hallett J. 1974. Nucleation and growth of bubbles at an ice-water interface. J. Glaciol. 13: 489–520.

Bengtsson L. 1996. Mixing in ice-covered lakes. Hydrobiologia 322: 91–97.

Brezinski D.P. 1983. Kinetic, static and stirring errors of liquid junction reference electrodes. Analyst 108: 425–442.

Byrne R.H. and Breland J.A. 1989. High precision multiwavelength pH determinations in seawater using cresol red. Deep-Sea Res. 36: 803–810.

Cole J.J., Caraco N.F., Kling G.W. and Kratz T.K. 1994. Carbon dioxide supersaturation in the surface waters of lakes. Science 265: 1568–1570.

Coyne P.I. and Kelley J.J. 1974. Carbon dioxide partial pressures in arctic surface waters. Limnol. Oceanogr. 19: 928–938.

Craig H., Wharton R.A. and McKay C.P. 1992. Oxygen supersaturation in ice-covered Antarctic lakes: Biological versus physical contributions. Science 255: 318–321.

DeGrandpre M.D., Hammar T.R., Smith S.P. and Sayles F.L. 1995. *In situ* measurements of seawater pCO_2. Limnol. Oceanogr. 40: 969–975.

DeGrandpre M.D., Hammar T.R., Wallace D.W.R. and Wirick C.D. 1997. Simultaneous mooring-based measurements of seawater CO_2 and O_2 off Cape Hatteras, North Carolina. Limnol. Oceanogr. 42: 21–28.

DeGrandpre M.D., Hammar T.R. and Wirick C.D. 1998. Short-term pCO_2 and O_2 dynamics in California coastal waters. Deep-Sea Res. II 45: 1557–1575.

DeGrandpre M.D., Baehr M.M. and Hammar T.R. 1999. Calibration-free optical chemical sensors. Anal. Chem. 71: 1152–1159.

Farmer D.M. 1975. Penetrative convection in the absence of mean shear. Quart. J. R. Met. Soc. 101: 869–891.

French C.R., Carr J.J., Dougherty E.M., Eidson L.A.K., Reynolds J.C. and DeGrandpre M.D. 2002. Spectrophotometric measurements of freshwater pH. Anal. Chim. Acta. 453: 13–20.

Herczeg A.L. and Hesslein R.H. 1984. Determination of hydrogen ion concentration in softwater lakes using carbon dioxide equilibria. Geochim. Cosmochim. Acta 48: 837–845.

Hesslein R.H., Rudd J.W.M., Kelly C., Ramlal P. and Hallard K.A. 1991. Carbon dioxide pressure in surface waters of Canadian lakes. In: Wilhelms S.C. and Gulliver J.S. (eds), Air-water mass transfer., pp. 413–431.

Juday R.E. and Keller E.J. 1980. A water quality study of Placid Lake and its drainages. MWRRC Report No. 110. Montana State University, Bozeman, Montana, USA.

Kling G.W., Kipphut G.W. and Miller M.C. 1992. The flux of CO_2 and CH_4 from lakes and rivers in arctic Alaska. Hydrobiologia 240: 23–36.

Kratz T.K., Cook R.B., Bowser C.J. and Brezonik P.L. 1987. Winter and spring pH depressions in northern Wisconsin lakes caused by increases in pCO_2. Can. J. Fish. Aquat. Sci. 44: 1082–1088.

Lemmin U. 1987. The structure and dynamics of internal waves in Baldeggersee. Limnol. Oceanogr. 32: 43–61.

Livingstone D.M. 1993. Lake oxygenation: Application of a one-box model with ice cover. Int. Revue ges. Hydrobiol. 78: 465–480.

Malm J., Bengtsson L., Terzhevik A., Boyarinov P., Glinsky A., Palshin N. et al. 1998. Field study on currents in a shallow, ice-covered lake. Limnol. Oceanogr. 43: 1669–1679.

Mathias J.A. and Barica J. 1980. Factors controlling oxygen depletion in ice-covered lakes. Can. J. Fish. Aquat. Sci. 37: 185–194.

Matthews P.C. and Heaney S.I. 1987. Solar heating and its influence on mixing in ice-covered lakes. Freshwat. Biol. 18: 135–149.

Millero F.J. 1979. The thermodynamics of the carbonate system in seawater. Geochim. Cosmochim. Acta 43: 1651–1661.

Nebaeus M. 1984. Algal water-blooms under ice-cover. Verh. Internat. Verein. Limnol. 22: 719–724.

Schindler D.W. 1971. Light, temperature, and oxygen regimes of selected lakes in the Experimental Lakes Area, northwestern Ontario. J. Fish. Res. Bd. Canada 28: 157–169.

Schindler D.W., Welch H.E., Kalff J., Brunskill G.J. and Kritsch N. 1974. Physical and chemical limnology of Char Lake, Cornwallis Island (75 degrees N lat.). J. Fish. Res. Bd. Canada 31: 585–607.

Stigebrandt A. 1978. Dynamics of an ice covered lake with through-flow. Nordic Hydrol. 9: 219–244.

Streebin L.E., Robertson J.M., Allen S.M., Heller W.B. and Westhoff J. 1973. Water quality study of the Clearwater River and selected tributaries. Lolo National Forest, USDA Forest Service, Missoula, Montana, USA.

Striegl R.G. and Michmerhuizen C.M. 1998. Hydrologic influence on methane and carbon dioxide dynamics at two north-central Minnesota lakes. Limnol. Oceanogr. 43: 1519–1529.

Weiss R.F. 1974. Carbon dioxide in water and seawater: The solubility of a non-ideal gas. Mar. Chem. 2: 203–215.

Welch H.E. and Bergmann M.A. 1985. Water circulation in small arctic lakes in winter. Can. J. Fish. Aquat. Sci. 42: 506–520.

Wetzel R.G. 1983. Limnology. 2nd edn. Saunders, New York, 767 pp.